Front. Struct. Civ. Eng. 2022, 16(4): 515–532
https://doi.org/10.1007/s11709-022-0814-4

RESEARCH ARTICLE

Detection of critical road roughness sections by trend analysis and investigation of driver speed interaction

Meltem SAPLIOGLU[a*], Ayse UNAL[b], Melek BOCEK[a]

[a] *Department of Civil Engineering, Suleyman Demirel University, Isparta 32260, Turkey*
[b] *Department of Civil Engineering, Siirt University, Siirt 56100, Turkey*
[*] *Corresponding author. E-mails: meltemsaplioglu80@gmail.com; meltemsaplioglu@sdu.edu.tr*

ABSTRACT Pavement roughness (IRI—International Roughness Index values) influence the stability of traffic movements both on intercity roads and urban roads. This study is to determine the exact locations of critical pavement roughness values that affect traffic motion stability and comfort in city centre highway arteries. Roughness data with 10 m intervals were collected on a 3140 m divided road containing three consecutive signalized intersections in the city centre arterial. These data were analysed using the distance-dependent Mann-Kendall trend analysis method and checkerboard model. The sections where roughness is important were determined at a 95% confidence interval. The results will show where future pavement improvements should be prioritized for municipalities and road maintenance engineers and will form a basis for the urban road management system.

KEYWORDS trend analysis, checkerboard model, IRI, driver speed

1 Introduction

The most important feature expected from flexible pavements, which are frequently used on highways, is to provide a structural service based on traffic loads and environmental effects. They should also provide a road surface which allows drivers to travel safely and comfortably within a certain speed range. In addition to these general principles, it is imperative that flexible pavements are long-lasting and sustainable, with the help of periodic maintenance and repairs [1]. Thanks to the pavement management system, road engineers and managers can meet those expectations. For appropriate maintenance and rehabilitation on urban roads, it is critical to identify the parts of the pavement requiring improvements. It is also necessary to identify areas requiring improving most in those developing countries where resources are limited. Therefore, pavement surface roughness, cracking, and rutting, etc., which are important key elements for performance indicators, should be examined separately [2].

Roughness, measured as the International Roughness Index (IRI), is one of the variables that best defines the asphalt pavement service level and user ratings [3]. It covers all of the wavelengths that are important for motor vehicles [4].

In the main arteries, which form the backbone of an urban transportation network, loss of strength is often observed in pavements, due to vehicle density, axle load, environmental and weather factors, and lack of maintenance. It is also known that increased deterioration and roughness in pavement conditions significantly influence driver behavior [5] and stability of traffic movement [6]. Studies have also shown that roughness linked to pavement conditions significantly affects road safety in pavements with low-speed limits, mean speed and variation of speed [7–9]. For instance, accident statistics indicate that multiple-vehicle crashes occur when IRI values are high and road surface maintenance is neglected [10–13].

There are prominent studies on the irregularity of urban road pavements, the deterioration of the coating layer and roughness. These studies generally focus on traffic flow, safety, pavement management and service-level interaction with the negative effects of deformed sections [14–17]. In addition to these, relations between drivers'

Article history: Received Nov 13, 2021; Accepted Dec 14, 2021

lane utilization and pavement condition have been studied [18–20]. Additionally, there are parameters that affect IRI values, such as traffic volume, time, and freeze-thaw, all of which have been effectively studied to date [21].

From a different point of view, our study is guided by the question: on which spatial points do road roughness vary along a road line in a main artery, given fixed pavement conditions, weather conditions and time period. In particular, the evaluation of pavement roughness (IRI) measurement is emphasized. There are very few studies conducted on finding locations of the pavement roughness that showed intense changes in city arterials [5,13]. Recognizing the high-roughness parts of urban road pavements to help make improvements is one of the steps needed to solve the safety problem in urban transportation networks and to operate pavement management systems efficiently.

The main purpose of our study, therefore, is to determine whether the roughness of the pavement is different in different lanes (right, middle, and left lanes) along the main artery. If there is an increasing trend of roughness, the study aims to show precisely in which segments it increases most. For this purpose, this study tries to determine the sections and lanes in which the roughness value is higher than the acceptable limits, using the Mann Kendall trend test method.

For an accurate measurement, IRI measurements were carried out under police supervision and using cruise control. In addition, the measurements were taken from road sections with similar pavement types and weather conditions, so that the IRI differences were not affected by the sub-ground and base-ground. Road sections with very similar traffic volumes were evaluated.

In the second part of the study, studies and standards related to roughness, speed and other parameter interactions were included. In the third part, the study area was introduced, the speed behaviors of drivers in different parts of the road line were assessed and separate IRI values were measured at 10 m intervals for each lane along the 4.140 km road line (round trip total). In the fourth part, the Mann-Kendall trend method is applied on a three-dimensional checkerboard to determine how IRI values change from the beginning of the measurement line towards the intersection centres and whether there is a trend of increase in high IRI values. A synthesis of results and discussion is then presented for future studies.

2 Overview of relevant past studies

2.1 Measurability of roughness

Understanding and measuring road roughness are key concerns in national and urban pavement systems [22]. Roughness is important because it affects the safety of road users, driving quality, as well as the remaining service life of the pavement due to loads from vehicles, especially heavy vehicles [23]. Roughness imposes undesirable vertical accelerations and other forces on drivers, thus contributing to an undesirable, uneconomical, unsafe, or uncomfortable drive [24]. Hence, IRI, which is recommended by the Directorate General of Highways and AASHTO, is one of the important parameters in determining the functional conditions of road pavement [25,26]. For this reason, if roughness can be measured, analysed, and located, a systematic program of rehabilitation or reconstruction can be implemented to provide efficient transportation facilities.

IRI was first introduced by the World Bank in a published report (1986) based on the International Road Roughness Experiment (IRRE). IRI is referred to as a quarter car model [27]. IRI is implemented in prEn 13036-5 [28] or ASTM E 1926-98 [29]. According to international standards, IRI represents the cumulative deviation from a smooth road surface in meters per km (or inches per mile). The General Directorate of Highways in Turkey uses IRI measurement values in the performance of road asphalt concrete research, in collaboration with the University of Texas Austin Highway and Transportation Research Center [30]. IRI measurements can be obtained using several measurement methods such as portable slope meters, dipstick, rolling-straight edge, profilograph, MERLIN, Hawkeye, response-type road roughness meters such as Roughometer NAASRA or Roughometer II and various other profile measuring instruments [31,32]. In recent years, smartphones have been used in other studies for IRI measurement, and real-time IRI measurements have been achieved, with good results [33,34].

The IRI values are expressed in meters per kilometre in Fig. 1(a) and a classification of pavement conditions based on IRI values is tabulated in Fig. 1(b) (Constraint values of Fig. 1(b) were used in this study.)

2.2 IRI's interaction with velocity and other parameters

The level of roughness that a vehicle is exposed to on an asphalt road generally affects the driving comfort, operating cost, and safety of the vehicle [35]. When examined in greater detail, it is evident that these effects depend also on vehicle characteristics (such as vehicle weight, suspension system, number, and type of wheels) and travel speed [4,36]. In addition, studies reveal that roughness is related to traffic volume, pavement type [36,37] the road's geometric features, such as the number of lanes, width, intersection status, and the drivers' behaviour in terms of negative or positive acceleration of vehicles [36,38–40].

In geometry-based measurements of roads, the geometric values are correlated with the dynamic movements

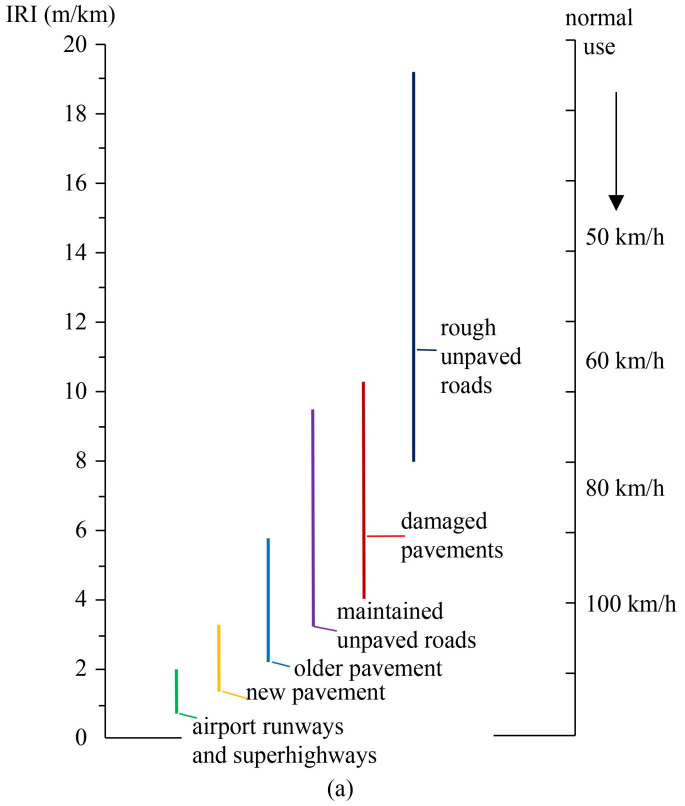

IRI value	category of road conditions
IRI ⩽ 2	very good
2 < IRI ⩽ 4	good
4 < IRI ⩽ 6	fair
6 < IRI ⩽ 8	poor
8 < IRI	very poor

(b)

Fig. 1 (a) IRI scale [25,27]; (b) criteria of pavement conditions based on IRI volumes [29,32].

and weights of the vehicle. The IRI value is accepted as a geometric measurement value and is associated with vehicle response [4]. Therefore, it should not be overlooked that when driving in normal environmental conditions, the roughness of the pavement is a factor that can affect driver behaviour and vehicle speed. The driver's responses in terms of acceleration and deceleration is just one example of roughness's effects on driver behaviour [39,41]. Additionally, roughness reduces the availability of some forces for controlling the vehicle, and so can affect driver behaviour [42]. Despite all this information, there are very few studies that examine the relationship between vehicle speed and roughness [43,44]. In one of these rare but rigorous studies, Yu and Lu [45] found that speed decreased by 0.84 km/h on average for each increase in IRI of 1578 cm/km.

In pavement conditions that significantly affect driving speed, there are significant economic losses in terms of capacity, time and comfort [43]. In capacity studies, it is not known to what extent roughness affects operating speed [46]. However, since parameters such as driver characteristics, vehicle characteristics, road characteristics, traffic characteristics and environmental characteristics affect speed differently for each region, it is necessary to study the speed-roughness relationship at least for each work area on a highway or city road.

The review of the literature shows that the measured roughness value varies depending on speed, vehicle characteristics and road geometries, requiring a constant speed measurement while measuring irregularities. It has been determined that the IRI measurement value limits in urban measurements are similar to the value limits for non-urban roads [35]. In addition, it is appropriate to use the same vehicle as a measurement tool along the entire road to ensure consistency of precision. For this reason, the same vehicle was used in the IRI measurements in our study, and the vehicle type and characteristics were kept constant. The measurements were taken on the same type of flexible pavement, under police supervision and using cruise control.

3 Materials, study area, and data collection

The study area is in Isparta city centre in the south of Turkey; SD Avenue is the main artery selected, which consists of flexible pavements. The roughness data, traffic volume data and speed data were collected. Figure 2 presents a satellite image showing the selected road line, signalized intersections and road line photographs. The following are the reasons for choosing this main artery.

- It is the busiest main artery passing through the city centre on the north south line, and carries heavy vehicle traffic. The high traffic volume provides a sufficiently large sample size of vehicles.
- It contains the central transit and stop points of the bus lines used as public transportation. The entrance to

Fig. 2 Study area SD Avenue and signalized intersections on road line (in Sparta, Turkey).

and exit from the road line of the intercity bus terminal is also on this street.

- It is the only connection road between SD University, which has 81,000 students, and the city centre, which has a population of 258000.
- It has a speed limit of 50 km/h; visible road surface signs and lane lines are available. Bicycle paths are separated from the main artery and do not affect vehicle traffic. However, it is known as the city center artery that has the highest rate of accidents [47].
- There are points at suitable angles and heights for taking camera shots.

There are three signalized intersection approaches with heavy traffic on the measured road line. Measurements were taken from the lanes on the round-trip route in the north-south direction of the road line at the signalized intersections called Aypa (Int. 1), Otogar (Int. 2), and Bellona (Int. 3). Measurements were carried out in two stages. In the first stage, speed and traffic volume data were collected; in the second stage, IRI values were taken to determine roughness.

3.1 Speed and traffic volume data collection

In intersection approaches and along the road line, velocity values were measured as average speed over the distance. For this, each lane was divided into zones (Zone 1, Zone 2, …, etc.), and each zone was divided into sections (1-a, 1-b, 1-c, 1-d, …, etc.). Zone and section lengths are given in Fig. 3. Lane widths are standardized at 2.75 m. The speed limit is 50 km/h in the selected sections. To accurately identify the roughness-affecting factors (e.g., whether there is an intersection, whether there is a bus stop or not), a road line containing sections with the same type of flexible pavement was selected. Cameras placed in each section in the measurement zones were operated simultaneously, and transition times between sections were obtained from one hour's worth of camera footage.

Changes in the speed of vehicles often reflect differences in the IRI values that affect ride quality [36]. This means that differences in vehicle speeds cause the IRI to feel different, and drivers may show different acceleration and deceleration behaviours according to changes in their perceived IRI values. However, in an urban intersection approach with a low-speed limit, it is expected that drivers in the green light crossing will behave the same for each lane in the same direction, and will pass without stopping at the intersection. If a driver in a neighbouring lane slows down while passing the intersection, the reason is that he will either turn or use the brake system to slow down. In light of this, only the speeds of the vehicles that were passing straight through during a green light were taken into consideration; vehicles that were slowing down due to a red light or turning were excluded from the data.

The approach speed of vehicles standing at red lights and turning vehicles are eliminated in order to understand whether there is an unevenness effect in vehicle speed changes. In the speed measurements for all lanes, only the velocities of the vehicles captured on camera while passing straight through during a green signal were considered.

To increase the sensitivity of the speed measurements, two yellow bands with certain spacing in the transverse direction were affixed on the road platform in the camera's field of view. The section lengths were thus seen more clearly when evaluating the camera images (Fig. 4). For a

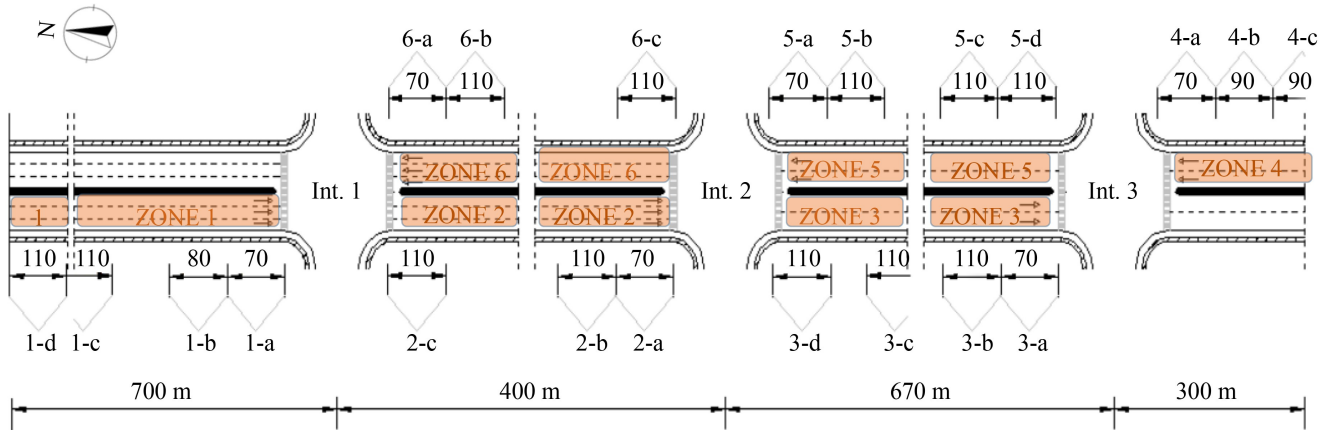

Fig. 3 Selected zone and section lengths for measurement.

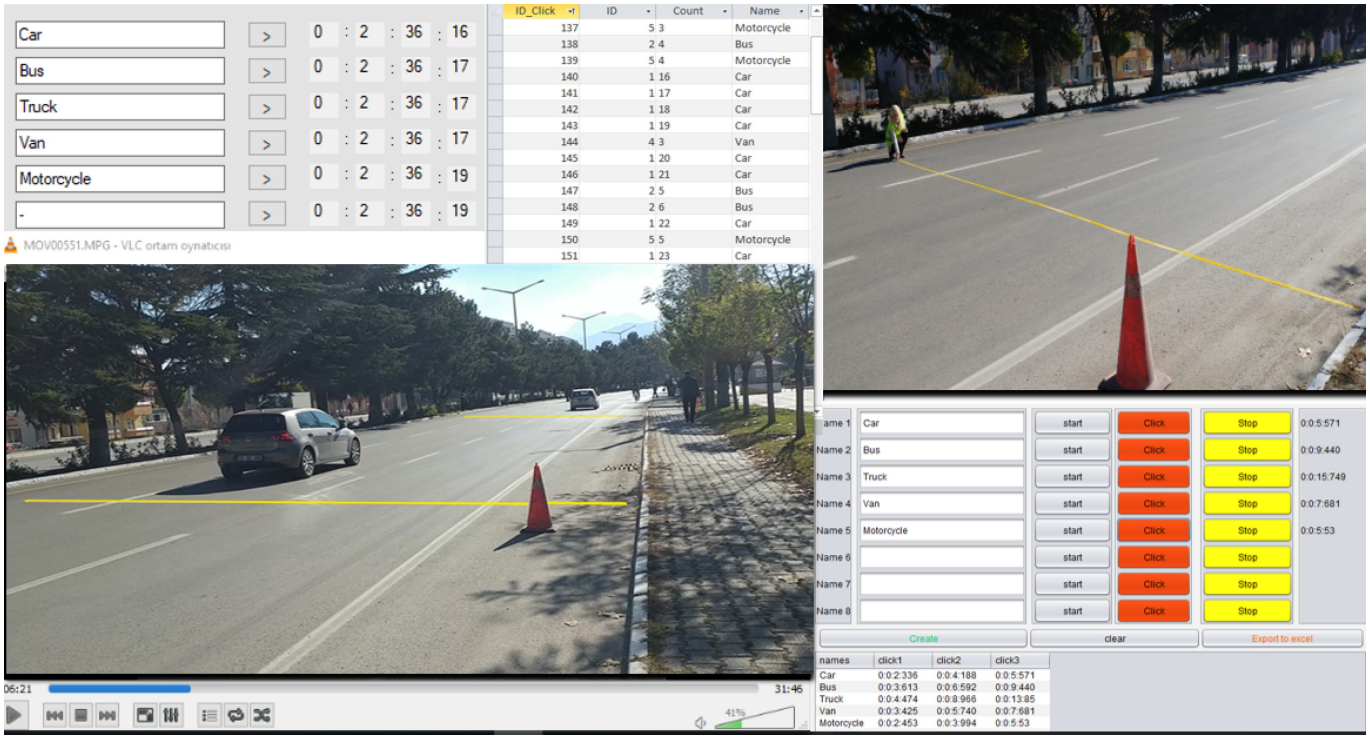

Fig. 4 Measurement of the average velocity values.

more precise evaluation, a program that calculates vehicle transition times from slowed camera images was written using Visual Basic and Java software. The resulting interfaces are given in Fig. 4. Thus, the average velocity values in the cross-section intervals could be calculated more precisely.

Observations were made during peak hours for traffic volume. Measurements were repeated when the road surface was dry road conditions, two days on weekdays and one day on weekends, three times in total. Vehicle types were considered in different traffic flow conditions, while counting by lane. The volume of vehicles was calculated by converting all vehicles to automobile equivalents (Table 1). In addition, the locations were determined GPS measurements, in order to account for features such as side road entries and exit locations, or bus stops on the right lane.

Average speed values for each of the a, b, c, and d sections and average traffic volume values on a lane-by-lane basis are given in Table 1.

3.2 Precise roughness data collection

The quality of the roughness condition data that informs the prioritization of pavement maintenance sections is valuable in facilitating decision-making in pavement management. In this study, an ARRB Roughometer II device was used for IRI measurements (Fig. 5(a)). In order to calibrate the roughness sensor of the Roughometer II device (Fig. 5(b)), a steel clamp, and a

Table 1 Intersection and zone numbers, average distance speeds and traffic volume data on the selected route

intersection	lane leng. (m)	zone No.	for speed measured			average speed (km/h)			traffic volume (v/h)		
			section No.	section leng. (m)	lane num.	right lane	middle lane	left lane	right lane	middle lane	left lane
Int.1	700	1	1-a	70	3	59.30	73.00	62.82	732	877	560
			1-b	80		62.40	72.47	65.80			
			1-c	110		39.50	52.25	75.42			
			1-d	110		55.60	59.32	73.84			
	400	6	6-a	70	3	32	–	42.5	425	576	224
			6-b	110		32.6	–	42.52			
			6-c	110		29.6	–	42.57			
Int.2	400	2	2-a	70	3	52.00	56.05	52.00	673	745	582
			2-b	110		52.60	55.00	54.34			
			2-c	110		49.60	48.52	61.13			
	670	5	5-a	70	2	34.3	–	32.47	775	–	462
			5-b	110		36.35	–	37.65			
			5-c	110		42.22	–	41.06			
			5-d	110		52.81	–	40.48			
Int.3	670	3	3-a	70	2	41.50	–	40.52	816	–	1014
			3-b	110		41.35	–	42.22			
			3-c	110		46.31	–	45.13			
			3-d	110		49.23	–	51.20			
	300	4	4-a	70	2	57.28	–	40.86	1066	–	1182
			4-b	90		41.18	–	38.92			
			4-c	90		33.51	–	38.23			

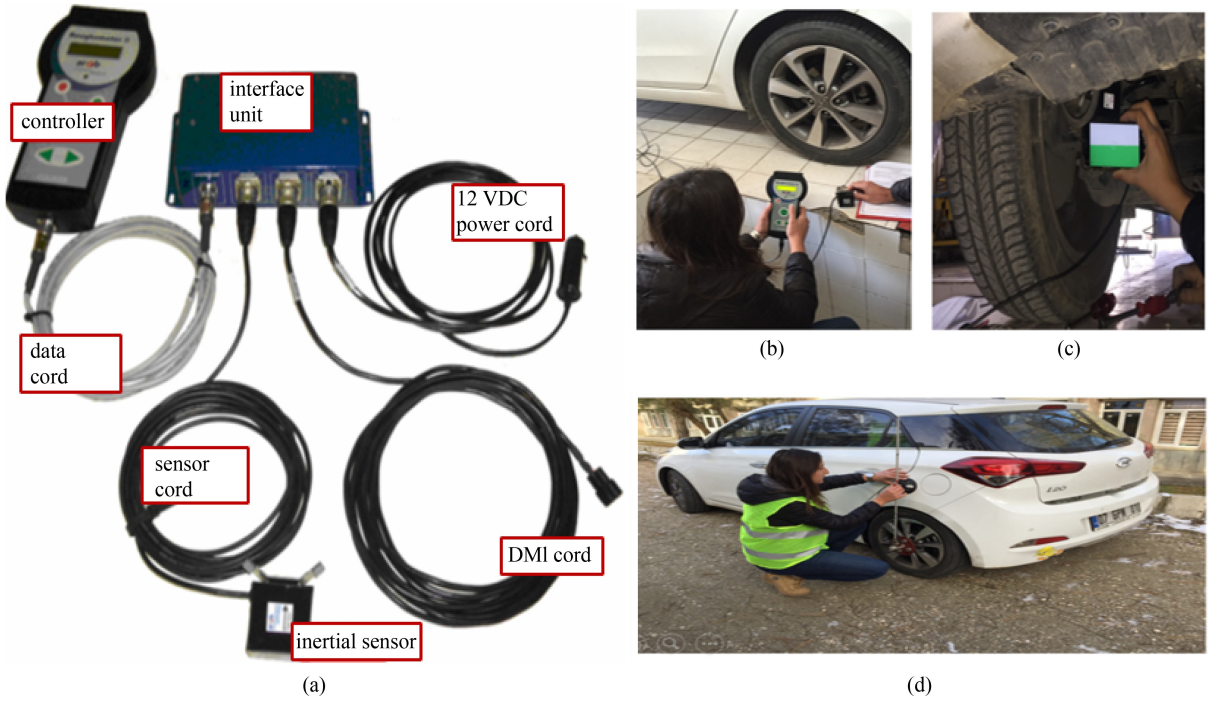

Fig. 5 (a) Roughometer II device; (b) vehicle axle connection; (c) axle connection balance control and (d) distance measurement connection.

Roughometer II sensor were attached to the suspension axle connected to the left rear wheel of the vehicle, the smoothness of the device was checked with a spirit level and the sensor cable was connected to the interface module inside the vehicle (Fig. 5(c)). A distance meter was mounted on the left rear wheel (Fig. 5(d)).

Once the control box was connected to the interface module, the measuring device was ready for use (Fig. 6(a)). In order to avoid damage to the device and to ensure accurate measurements, the device was removed after measurements and was recalibrated for each new measurement. As a response-type road roughness measurement system, the Roughometer II not only measures accumulated axle displacement, which is the "m/km" deviation of the road surface, but also assigns a location for each measurement value via GPS connection. Graphs containing the movement of the axle body versus the travel time were obtained as output, and longitudinal road profile readings were facilitated by GPS coordinates.

IRI measured values change according to vehicle speed [48]. Vehicle cruise control was used to eliminate the effect of acceleration in the measuring vehicle. A constant speed of 50 km/h was maintained during the measurement. Measurements taken from each zone were repeated on three different days to reduce error that may occur as a result of physical differences in the road environment.

The data were taken during early morning hours, between 03:00 and 05:00, when the traffic signals are switched to flash and there is no heavy traffic, in order to be able to take measurements with a constant speed (Fig. 6(b)). In addition, in order to ensure a safe constant speed while crossing intersections, measurements were carried out with the assistance of a police team from the Isparta Traffic Inspection Directorate (Fig. 6(c)). Thus, the measurements were carried out precisely, safely, and at a constant speed.

Fig. 6 (a) Roughometer control box usage; (b) midnight measurements; (c) meeting the team provided by the Isparta Traffic Inspection Directorate.

IRI values were obtained by measuring the road profile for all road sections of totally 3.140 km length. IRI measurement values are presented in the figures in the results and evaluations section.

4 Determining the critical roughness sections using the Mann Kendall trend test

This study aimed to identify the sections with high IRI values that are thought to affect driver speed changes in urban roads. For this, 7570 IRI values showing positional changes depending on the distance were first measured separately for each lane. Trend analysis was used for evaluation. Several parametric and non-parametric tests were applied in trend analysis studies. Nonparametric trend tests do not require normality assumptions in data but do require data to be independent [49,50] and, rather than actual measurements, their ranks can be taken into consideration [51]. The ranks used in Fig. 1(b) were taken into consideration to evaluate the IRI data collected in our study, using a trend test.

Although IRI trends can be identified by lots of trend methods, the importance of the trend, i.e., how the roughness changes, is not easily ascertained. Effective and efficient pavement management requires determining not only the IRI values but also the factors that are interacting with them. For this purpose, the present study surveys the IRI value depending on the distance at the sections where driver speeds increase or decrease along the route. Since the IRI measurement sections and velocity measurement sections overlap, both the sections where the unevenness tends to increase separately for each strip and the changes in the average velocity values in these sections were observed. The significance level of the increasing trend values of the IRI data series was determined at every 10 m at a 95% confidence interval. For this, the widely used [52, 53] Mann Kendall trend test was applied.

The Mann Kendall trend test does not make any assumptions about data distribution. In this procedure, a null hypothesis test is set up to see if a trend exists in the series. In a case where the values obtained in the test exceed certain limit values (if the null hypothesis is rejected), the presence of a trend can be inferred. While performing the analysis, the data series are as x_1, x_2, ..., x_n, (x_i, x_j) which can be thought of as the starting point (x_1) and the ending point (x_n) along IRI measured road. If the condition $i < j$ is satisfied for each $x_i < x_j$ of these pairs, the value of P is increased by one. In the opposite case, M is increased for $x_i > x_j$. The test statistic is defined as $S = P - M$ [49,54]. For $n > 10$, the Kendall correlation

coefficient is calculated as follows (Eqs. (1) and (2)).

$$\mu_s = 0 \; ve \; \sigma_s = \sqrt{n(n-1)(2n+5)/18}, \tag{1}$$

$$\frac{s-1}{\sigma_s} s > 0, \; Z = 0, \; s = 0, \; \frac{s+1}{\sigma_s} s < 0. \tag{2}$$

If the obtained Z value is smaller than the α number corresponding to the $Z/2$ value in the normal distribution, the hypothesis is accepted, which in turn implies that there is no trend. If, on the other hand, the Z value is greater than the α value corresponding to $Z/2$, the hypothesis is rejected, and the presence of a trend is inferred. In cases where there is a trend, a positive S value indicates an upward trend, whereas a negative value for S indicates a downward trend [55].

The most common problem with the Mann Kendall method, which is generally used as a trend determination procedure for time series, is that different trend formations can be encountered in series taken in different time periods [56]. Our study encountered this problem in different parts of the cross-section lengths in trend research based on distance. For example, when looking at the trend in Zone 1 with 71 IRI data, all data between 1 and 71 are analysed and a corresponding trend is observed. In such a case, a single trend could be obtained based on all points between the start and end points. However, this number of data may differ between the 2nd and 70th data or between the 30th and 50th data. In other words, trend changes occurring in different segments go unnoticed whereas, ideally, all possible distance-dependent trend change possibilities should be considered. Various methods have been developed in studies conducted so far to solve this problem. One of these involves representing the Mann-Kendall trend method on a three-dimensional checkerboard [57,58], which was also used in our study. This method makes it easy to find all significant trend probabilities. The flow chart of the program, written in MadLab to automate this method and display it on the checkerboard, is as in Fig. 7.

5 Results and evaluations

In the display of the trend values on the three-dimensional checkerboard, the confidence intervals of the trends of the data taken in different distance segments were determined. In previous studies [57,58], the checkerboard-Mann Kendall trend testing method was used as the trend testing procedure for time series. It was used in this study for all test results obtained from different cut intervals in determining trends based on distance. In doing so, intervals of at least 10 data were used, which is the minimum requirement for a trend. Thus, with the checkerboard method, it was possible to apply the Mann Kendall test 1352 times for Zone 1 with 61 data. Similarly, for each of the different section lengths (Zone 1: 700 m; Zone 2: 400 m; Zone 3: 670 m; Zone 4: 300 m; Zone 5: 670 m; Zone 6: 400 m), the trend of IRI values measured every 10 m between sections of at least 100 m was determined. In addition, for easier analysis, software previously developed with MatLab [58] was used.

Figure 8 shows the three-lane Zone1 section in Intersection 1 that shows the comparative graphical data created for only the distance-dependent IRI values for the right lane and the varying speed averages depending on the distance. The locations of the two bus stops in the right lane in the section examined on the graphic are also shown.

To understand whether there is an increase in trends in the IRI values that vary depending on distance in the right lane, shown in Fig. 8, the trend was checked for each interval (for 10 m intervals) and 1352 Mann-Kendall tests were conducted. 126 of them show an increasing trend at a 95% confidence interval. MatLab software was used effectively to implement the method quickly and automatically.

In Zone 1, the significance level of the trend increased at the parts of the bus stops in the right lane and the places at the intersection of the 610th meter where junction arms are intersected as seen on the checkerboard (Fig. 9). The sections where normal trend increase values are seen in Fig. 9(a) were assessed using a colour scale. In Fig. 9(b), the ones that fall within the 95% confidence interval of these increases are shown in dark red. In Fig. 9(a), it is seen that trend existence is always present compared to the beginning but could not be proven with a 95% confidence interval. While the trend increase was significant between the beginning and the first bus stop in Zone 1, there was no significant tendency in the IRI increase between the beginning and the second bus stop. However, when all data are compared with the intersection approach and the first bus stop approach,

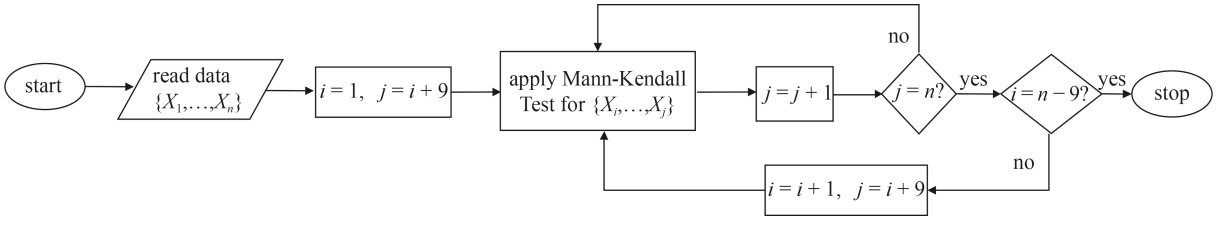

Fig. 7 Model flow diagram.

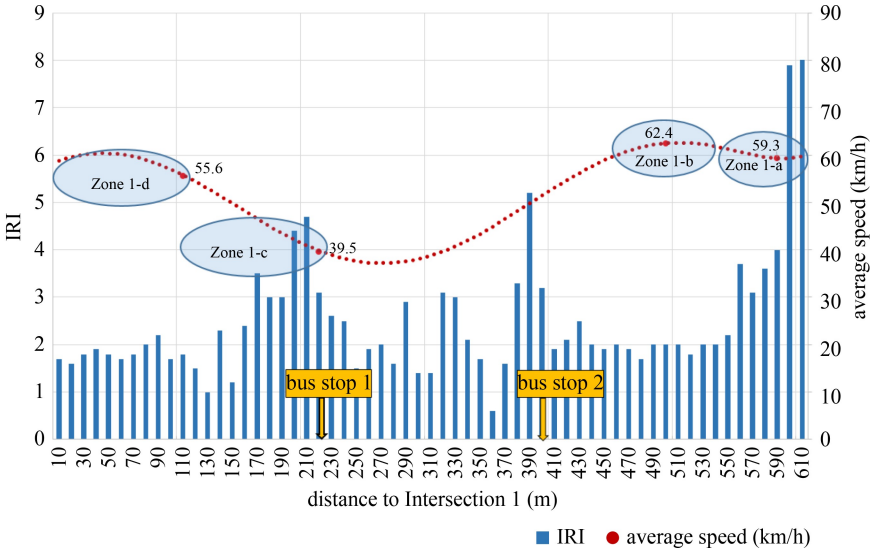

Fig. 8 Zone 1 IRI values for the right lane and the varying speed averages depending on distance.

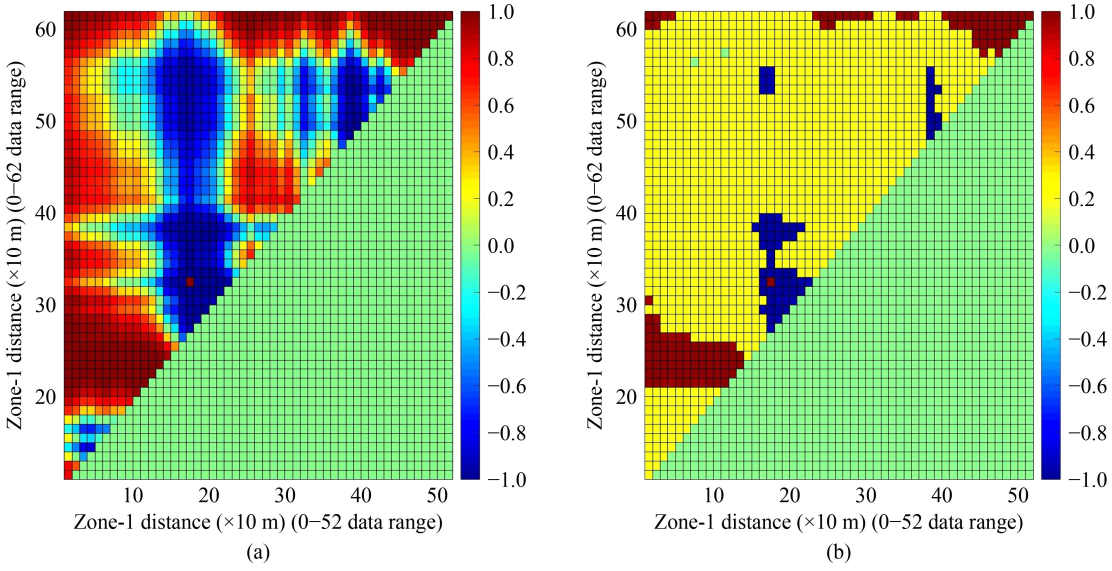

Fig. 9 (a) Intersection1-Zone1 on checkerboard model-trend analysis demonstration of IRI values normal trend changes; (b) trend changes for IRI values at 95% confidence interval.

Fig. 9(b) shows that the trend presence found is also significant for the second bus stop. Trend values within the 95% confidence interval, as in Fig. 9(b), should be preferred in order to statistically prove the trend increases for all sections, instead of the normal trend changes chart as seen in Fig. 9(a). For this, while interpreting other lanes' analysis results, graphs created for the 95% confidence interval are used.

The analyses for Zone 1's right lane, which are illustrated in Figs. 8 and 9, are also performed for all measured lanes and sections (Zones 2–6) along the road line in Figs. 10–15.

Both in Intersection 1-Zone 1's middle lane between the 250th and 290th m and in Intersection 2-Zone 2's middle lane have buses that switch from the right lane to the left lane (bus stop is adjacent to the right lane). According to the checkerboard method, the significance level of this increase in IRI values due to the acceleration effect of the vehicles and the bus is especially important at the exit of the bus stops (Fig. 10, Intersection 1-Zone 1-middle lane-b). When approaching the intersection centre in the middle lane, the significance level of the IRI increase is not found to be significant at the 95% confidence interval. In the left lane, both a decrease in speed along the road line and an increase in IRI on the intersection centre approach are seen. There is a continuity from high speed to low speed in the left lane. However, as stated before in the data collection phase, our data are restricted to those obtained during green lights for vehicles. This accounts for the deceleration

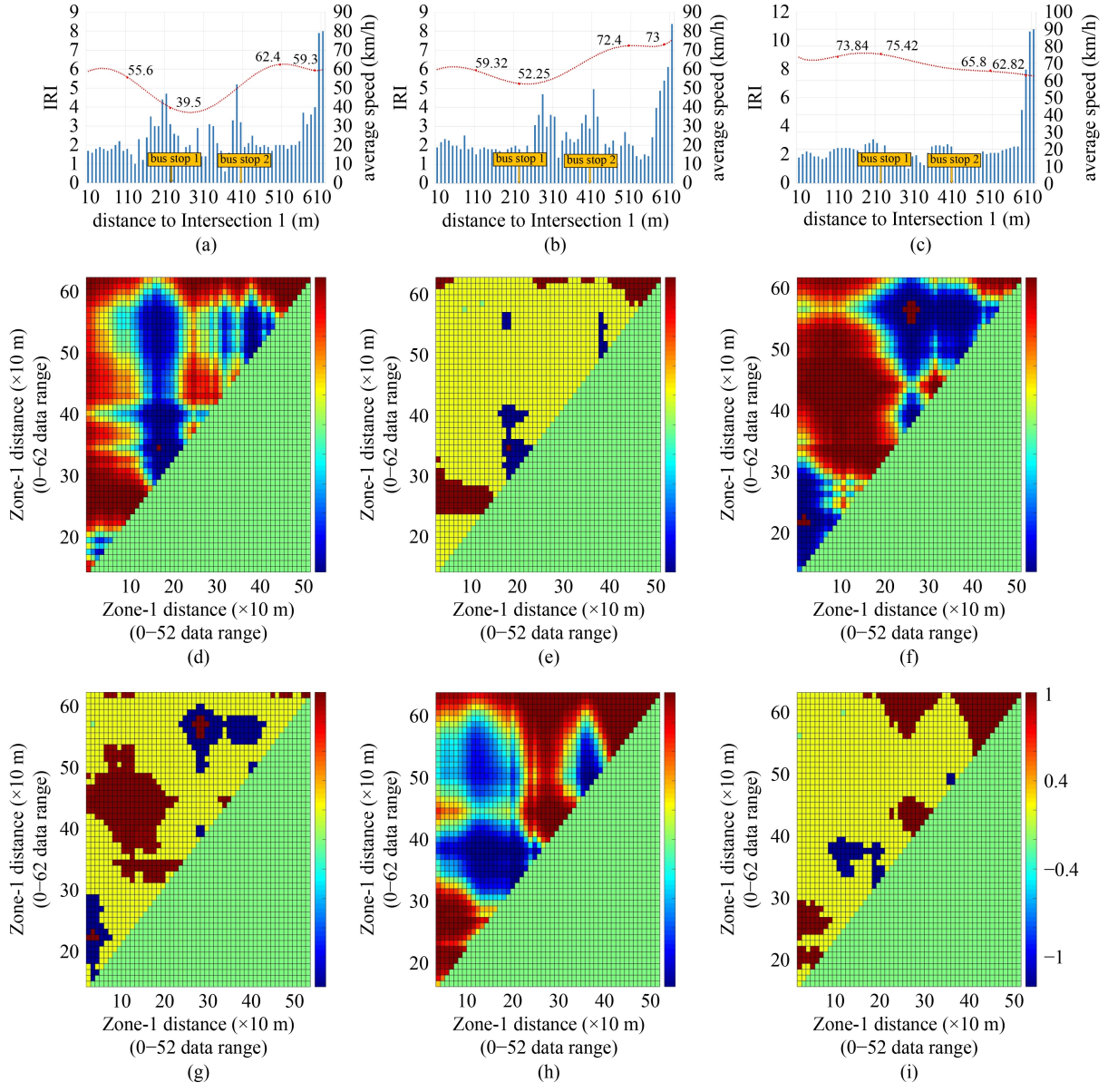

Fig. 10 Intersection 1-Zone 1: (a) the distance-dependent IRI values and speed averages graph for right lane; (b) the distance-dependent IRI values and speed averages graph for middle lane; (c) the distance-dependent IRI values and speed averages graph for left lane; (d) IRI values normal trend changes for right lane; (e) trend changes for IRI values at 95% confidence interval for right lane; (f) IRI values normal trend changes for middle lane; (g) trend changes for IRI values at 95% confidence interval for middle lane; (h) IRI values normal trend changes for left lane; (i) trend changes for IRI values at 95% confidence interval for left lane.

effect needed for left turns. This situation caused a significant increase in IRI values (Fig. 10, Intersection 1-Zone 1-left lane).

There is also a bus stop in the Intersection 2-Zone 2 right lane. In Zone 2, the bus stop exit section IRI values are high on the graph. In the checkerboard model, the trend significance value of these parts is very high. Speed changes are very low in the intersection approach. Drivers are mostly moving steadily at low speeds. Accordingly, the trend increase in IRI values within the centre of the right lane intersection is not at a significant level. In addition, just like the intersection 1-Zone 1, the bus stop exit point is in the middle lane in the intersection 2-Zone 2; In the left lane, especially in the intersection-centre approach, the increase in IRI trend values reached significant levels at the 95% confidence interval (Fig. 11).

Other sections are two-lane roads (Figs. 12–15). On two-lane road sections, traffic average speed values are lower in the right lane. When Zones 3–6 were examined, it was seen that the IRI values at 95% confidence interval in the right lane in the intersections are not too high for the limit values in the literature. In the left lane, there is an IRI trend increase in the intersection centre approach.

In areas containing bus stops, the increases in IRI trend values in both the right and left lanes were significant at the 95% confidence interval.

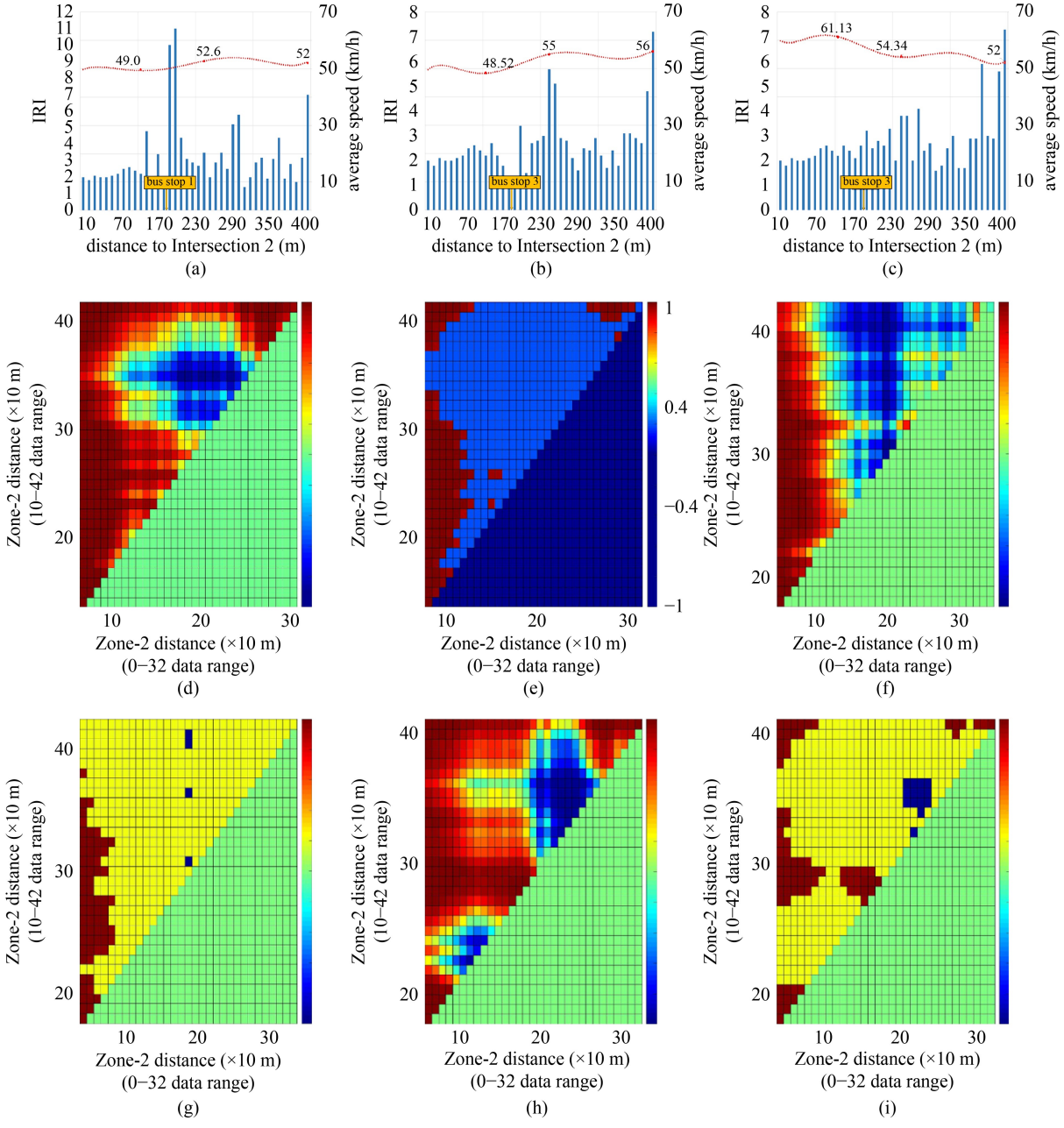

Fig. 11 Intersection 2-Zone 2: (a) the distance-dependent IRI values and speed averages graph for right lane; (b) the distance-dependent IRI values and speed averages graph for middle lane; (c) the distance-dependent IRI values and speed averages graph for left lane; (d) IRI values normal trend changes for right lane; (e) trend changes for IRI values at 95% confidence interval for right lane; (f) IRI values normal trend changes for middle lane; (g) trend changes for IRI values at 95% confidence interval for middle lane; (h) IRI values normal trend changes for left lane; (i) trend changes for IRI values at 95% confidence interval for left lane.

6 Conclusions and suggestions

The objective of this paper was to demonstrate usage of IRI in urban arterials for finding the locations of areas with high values of roughness and for understanding links with driver behavior. It showed that trend analysis can be used to discriminate the roughness level on the pavement of urban arterials by identifying features that contribute to roughness.

In accordance with the purpose of this article, places where the roughness variation is high were identified and the reasons for the increases were investigated. In addition, speed variations were examined to understand changes in driver behavior. Thus, the effect of the presence of IRI on the routes of the urban arterial roads has been examined.

Since it is known that measuring IRI values at different speeds gives erroneous results, this study's measurements were taken at a constant speed. The reliability of the data collected has been further increased by taking

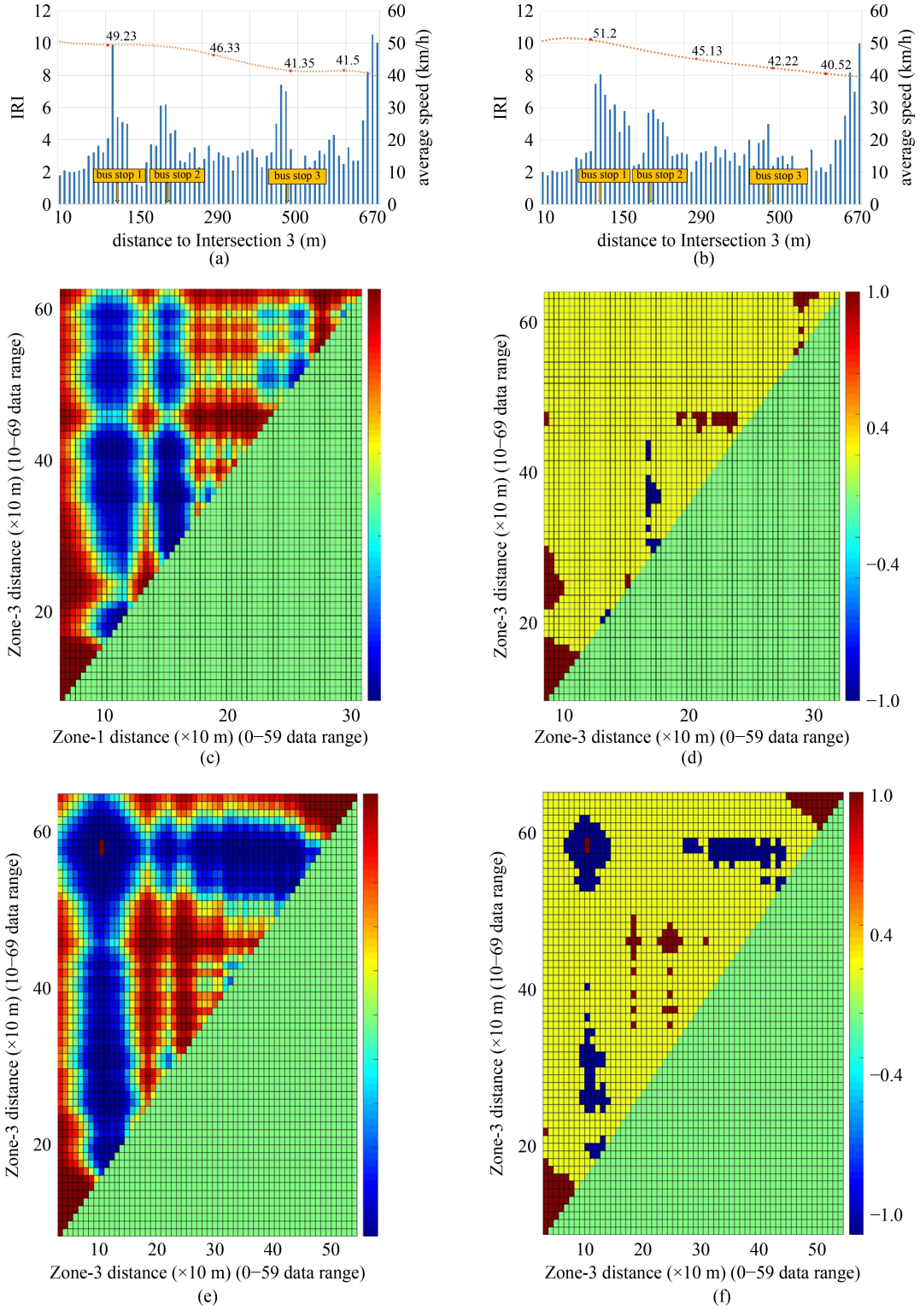

Fig. 12 Intersection 3-Zone 3: (a) the distance-dependent IRI values and speed averages graph for right lane; (b) the distance-dependent IRI values and speed averages graph for left lane; (c) IRI values normal trend changes for right lane; (d) trend changes for IRI values at 95% confidence interval for right lane; (e) IRI values normal trend changes for left lane; (f) trend changes for IRI values at 95% confidence interval for left lane.

measurements with the same vehicle during hours when the traffic is almost non-existent, and with assistance from traffic police.

The changes in the trend values of the IRI measurement values depending on distance were evaluated by drawing graphs along path lines and using the checkerboard-Mann

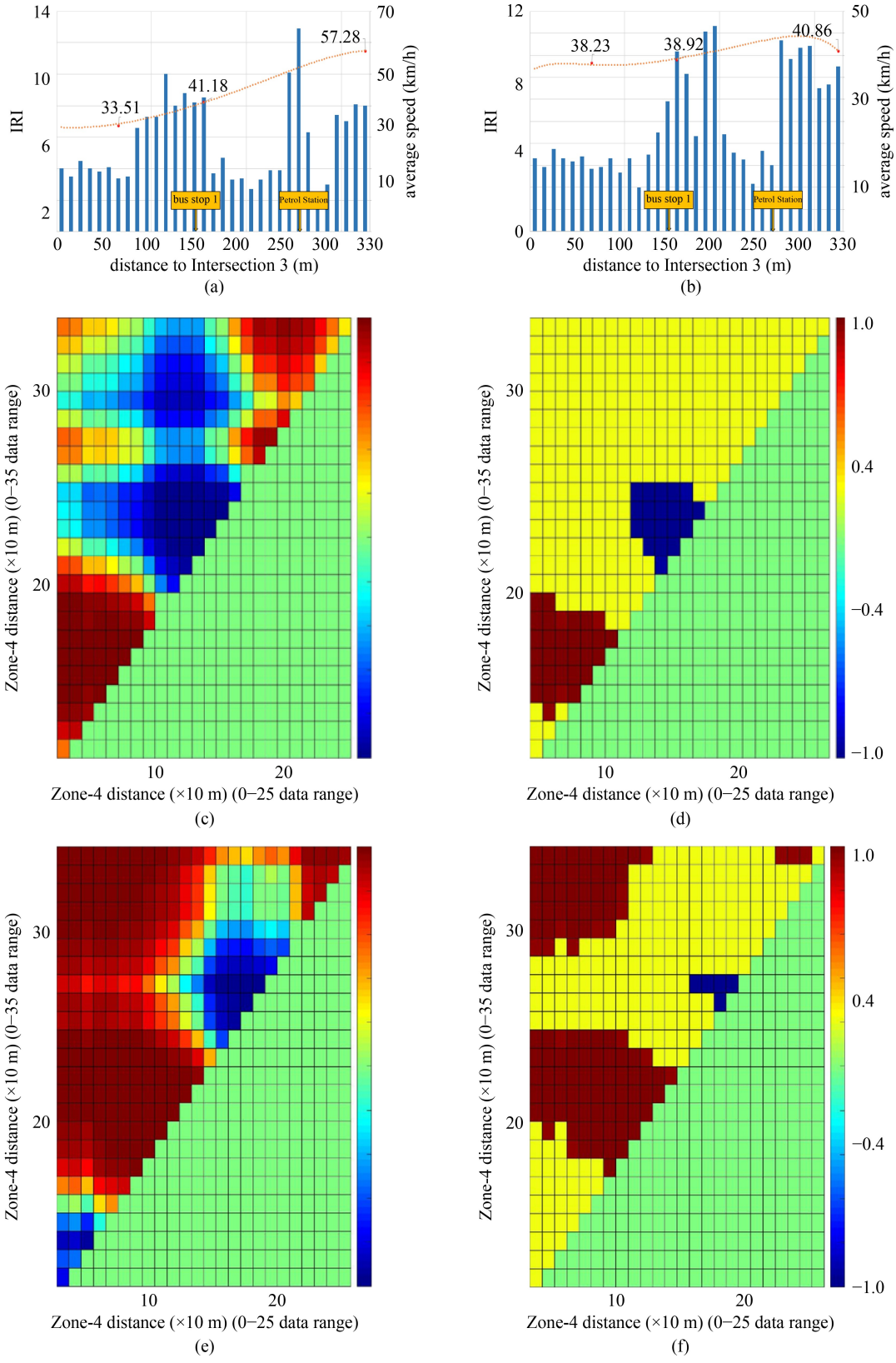

Fig. 13 Intersection 3-Zone 4: (a) the distance-dependent IRI values and speed averages graph for right lane; (b) the distance-dependent IRI values and speed averages graph for left lane; (c) IRI values normal trend changes for right lane; (d) trend changes for IRI values at 95% confidence interval for right lane; (e) IRI values normal trend changes for left lane; (f) trend changes for IRI values at 95% confidence interval for left lane.

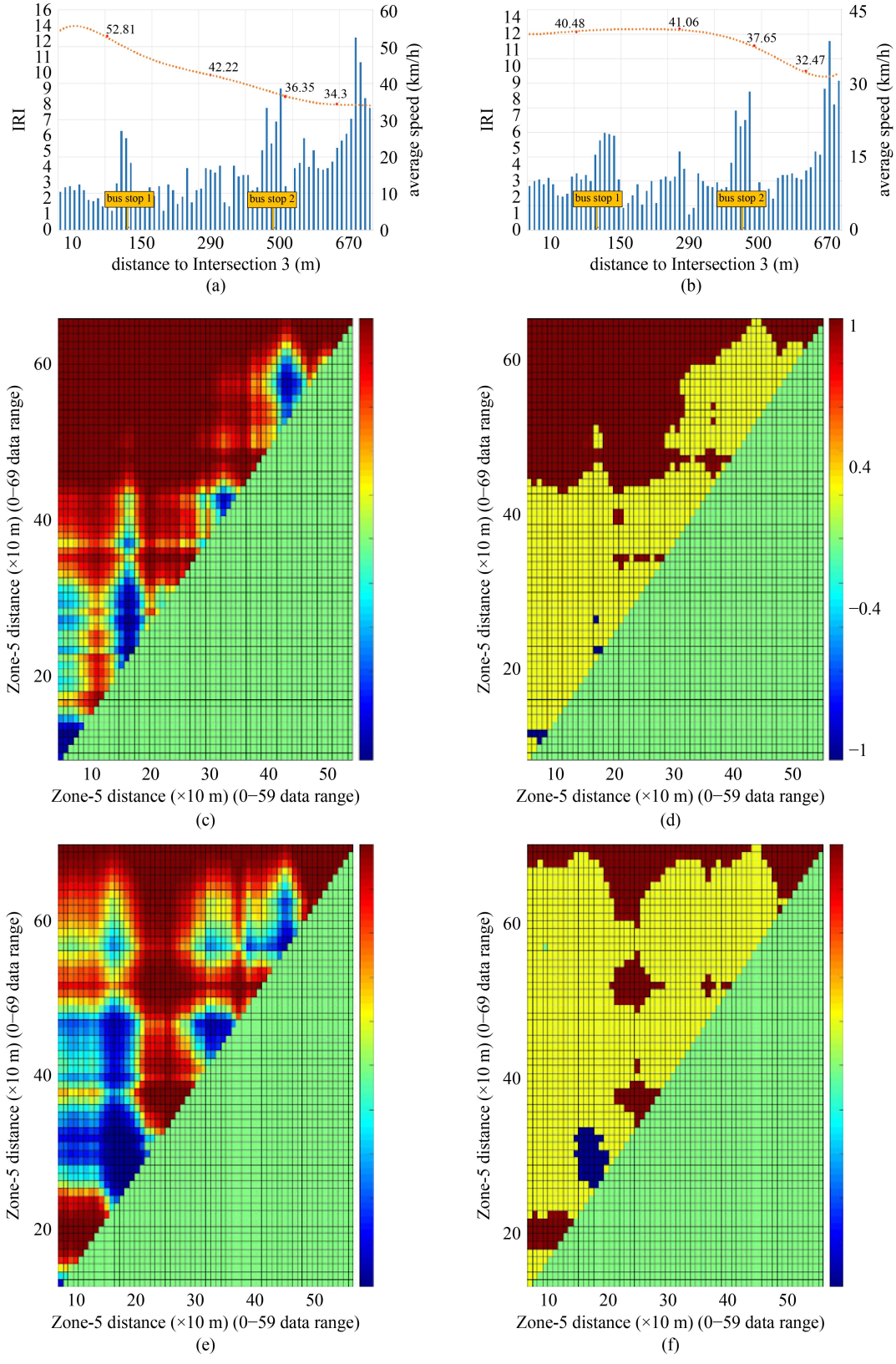

Fig. 14 Intersection 2-Zone 5: (a) the distance-dependent IRI values and speed averages graph for right lane; (b) the distance-dependent IRI values and speed averages graph for left lane; (c) IRI values normal trend changes for right lane; (d) trend changes for IRI values at 95% confidence interval for right lane; (e) IRI values normal trend changes for left lane; (f) trend changes for IRI values at 95% confidence interval for left lane.

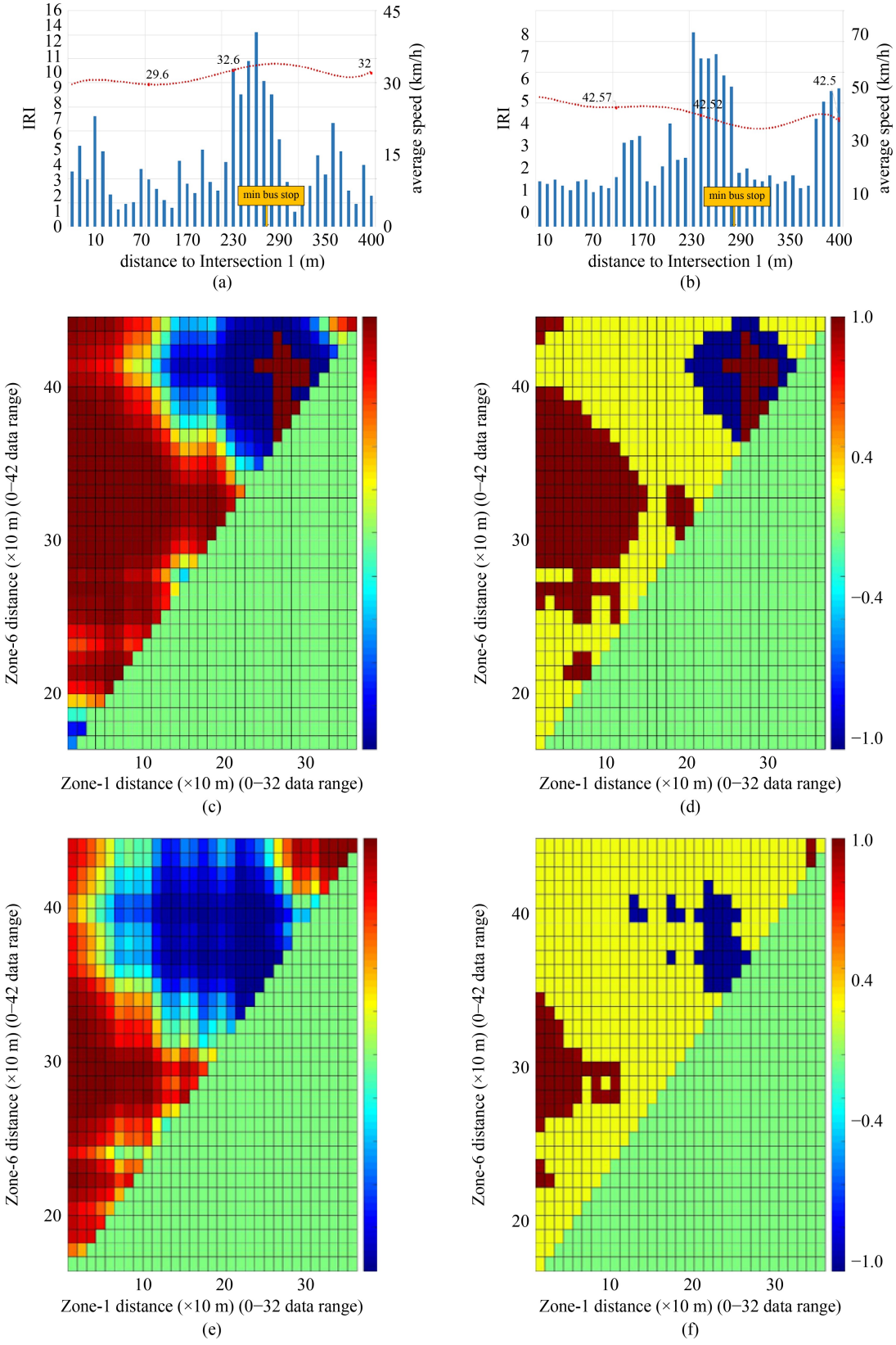

Fig. 15 Intersection1-Zone 6: (a) the distance-dependent IRI values and speed averages graph for right lane; (b) the distance-dependent IRI values and speed averages graph for left lane; (c) IRI values normal trend changes for right lane; (d) trend changes for IRI values at 95% confidence interval for right lane; (e) IRI values normal trend changes for left lane; (f) trend changes for IRI values at 95% confidence interval for left lane.

Kendall trend method. The method was used to determine the trend of change of IRI values that differ depending on the distance, which was assessed every 10 m in the sections between intersections and in different lanes. The biggest advantage of using the checkerboard method is that the trend of change of IRI values at different cut lengths and different coordinates can be determined within the 95% confidence interval, which is of great importance.

In the interpretation of the measured unevenness values in road sections and intersection approaches on the three-dimensional checkerboard, the beginning of each zone is considered as the beginning of the measurement point (zero distance). It has been possible to evaluate the IRI trend change values depending on distance with precise coordinates and to correlate them with the variations of average vehicle speeds with distance. The study determined that the segments with a rising trend in IRI values in the 95% confidence interval significantly affect drivers' behavior as regards speed.

According to the results obtained, the IRI change generally varies according to the right and left lanes of the road, and, further, is affected by the presence of a middle lane. The presence of bus stops affects the trend change in IRI values, as do intersection approaches. Although IRI trends at intersection approaches tend not to be very significant, bus stop approaches exhibit very significant IRI trend elevations. Interestingly, while bus stops increase IRI values in the right lane, there is also a trend of increasing IRI values in the middle lane toward the end of the bus stop. This supports the idea that bus stops should be located of road bus stops. If there are not enough additional lanes to make this possible, bus stop pavements should be reinforced by the use of more robust materials in the right and middle lanes.

As expected, there are also changes in IRI values in intersection approaches. However, these changes are not as high as those around bus stops. It is seen that results such as these are necessary for determining the places where pavement improvement should be made in main urban arteries. The study also demonstrated that distance-based trend analysis and the checkerboard-Mann Kendall method constitute a useful and quick decision-making method for practitioners in future improvement studies and sustainable pavement management.

References

1. Atahan A, Buyuk M, Malkoc G, Diez J. Safety of road work zones: European and the US perspective. In: 6th Eurasphalt & Eurobitume Congress. Prague: Czech Republic Publication, 2016: 1−3
2. Janani L, Dixit R K, Sunitha V, Mathew S. Prioritisation of pavement maintenance sections deploying functional characteristics of pavements. International Journal of Pavement Engineering, 2020, 21(14): 1815−1822
3. Ragnoli A, De Blasiis M R, Di Benedetto A. Pavement distress detection methods: A review. Infrastructures, 2018, 3(4): 58
4. Gillespie T D. Everything you always wanted to know about the IRI, but were afraid to ask! In: Road Profile Users Group Meeting. Nebraska: The University of Michigan Transportation Research Institute, 1992: 22−24
5. Unal A, Saplıoğlu M, Böcek M. Evaluation of the interaction of pavement unevenness and driver behavior in the signalized intersection approach. Academic Perspective Procedia, 2018, 1(1): 918−928 (in Turkish)
6. Han X, Xiang Q, Leng H. Evaluating the effect of freeway pavement conditions on traffic flow stability. In: 11th International Conference of Chinese Transportation Professionals (ICCTP). Nanjing: ASCE, 2011: 1925−1933
7. Chan C Y, Huang B, Yan X, Richards S. Investigating effects of asphalt pavement conditions on traffic accidents in Tennessee based on the pavement management system (PMS). Journal of Advanced Transportation, 2010, 44(3): 150−161
8. Li Y, Liu C, Ding L. Impact of pavement conditions on crash severity. Accident Analysis and Prevention, 2013, 59: 399−406
9. Kırbaş U, Karaşahin M. Investigation of ride comfort limits on urban asphalt concrete pavements. International Journal of Pavement Engineering, 2018, 19(10): 949−955
10. Al-Masaeid H R. Impact of pavement condition on rural road accidents. Canadian Journal of Civil Engineering, 1997, 24(4): 523−531
11. Cairney P, Bennett P. Relationship between road surface characteristics and crashes on Victorian rural roads. In: 23rd ARRB Conference. Adelaide: Transportation Research Board, 2008
12. Chan C Y, Huang B, Yan X, Richards S H. Effects of asphalt pavement conditions on traffic accidents in Tennessee utilizing pavement management system. In: Transportation Research Board 88th Annual Meeting. Washington, D.C.: Transportation Research Board, 2009
13. Hussein N, Hassan R. Surface condition and safety at signalised intersections. International Journal of Pavement Engineering, 2017, 18(11): 1016−1026
14. Hunt P D, Bunker J M. Road performance studies using roughness progression & pavement maintenance costs. In: Queensland Department of Main Roads Roads System and Engineering Forum. Brisbane: QUT ePrints, 2002
15. Ben-Edigbe J, Ferguson N. Extent of capacity loss resulting from pavement distress. Proceedings of the Institution of Civil Engineers-Transport, 2005, 158(1): 27−32
16. Ben-Edigbe J, Mashros N, Minhans A. Exploration of trapezoidal flowrate contractions resulting from pavement distress. Journal of Emerging Trends in Engineering and Applied Sciences, 2011, 2(2): 351−354
17. Sengoz B, Topal A, Tanyel S. Comparison of pavement surface texture determination by sand patch test and 3D laser scanning. Periodica Polytechnica-Civil Engineering, 2012, 56(1): 73−78
18. Gunay B. An investigation of lane utilisation on Turkish highways. Proceedings of the Institution of Civil Engineers-Transport, 2004, 157(1): 43−49

19. Yousif S, Al-Obaedi J, Henson R. Drivers' lane utilization for United Kingdom motorways. Journal of Transportation Engineering, 2013, 139(5): 441−447
20. Aydin M M, Topal A. Effect of road surface deformations on lateral lane utilization and longitudinal driving behaviours. Transport, 2016, 31(2): 192−201
21. Guo S, Dai Q, Hiller J. Investigation on the freeze-thaw damage to the jointed plain concrete pavement under different climate conditions. Frontiers of Structural and Civil Engineering, 2018, 12(2): 227−238
22. Shafizadeh K R, Mannering F L, Pierce L M. A Statistical Analysis of Factors Associated with Driver-perceived Road Roughness on Urban Highways. Olympia: Washington State Department of Transportation, 2002
23. King B A. The effect of road roughness on traffic speed and road safety. Bachelor of Civil Engineering project. Queensland: University of Southern Queensland, 2014
24. Hudson W R. Road Roughness: Its Elements and Measurement. Los Angeles, CA: SAGE Publishing, 1981
25. Samsuri S, Surbakti M, Tarigan A P, Anas R. A study on the road conditions assessment obtained from international roughness index (IRI): Roughometer Vs Hawkeye. Simetrikal: Journal of Engineering and Technology, 2019, 1(2): 103−113
26. AASHTO. Guide for Design of Pavement Structures. Washington, D.C.: American Association of State Highway and Transportation Officials, 1993
27. Sayers M W, Gillespie T D, Queiroz C A V. The international road roughness experiment: A basis for establishing a standard scale for road roughness measurements. Transportation Research Record: Journal of the Transportation Research Board, 1986: 76−85
28. CEN. Road and Airfield Surface Characteristics, Test Methods. Part 5: Determination of Longitudinal Unevenness Indices. Brussels: European Committee for Standardization, prEN 13036–5, 2015
29. ASTM E1926-08. Standard Practice for Computing International Roughness Index of Roads from Longitudinal Profile Measurements. West Conshohocken, PA: ASTM International, 2008
30. Usluogullari O F, Yildirim Y, Culfik M S. Evaluatıon of the performance of asphalt concrete roads usıng internatıonal roughness index (Irı) values. In: National Asphalt Symposium and Exhibition. Ankara: Turkish General Directorate of Highways, 2013, 27–28 (in Turkish)
31. Kırbaş U. IRI sensitivity to the influence of surface distress on flexible pavements. Coatings, 2018, 8(8): 271
32. Hasibuan R P, Surbakti M S. Study of pavement condition index (PCI) relationship with international roughness index (IRI) on flexible pavement. MATEC Web of Conferences, 2019, 258: 03019
33. Zhang Z, Zhang H, Xu S, Lv W. Pavement roughness evaluation method based on the theoretical relationship between acceleration measured by smartphone and IRI. International Journal of Pavement Engineering, 2021: 1−17
34. Hossain M I, Tutumluer E. Nikita, Grimm C. Evaluation of android-based cell phone applications to measure international roughness index of rural roads. In: International Conference on Transportation and Development 2019: Smarter and Safer Mobility and Cities. Reston, VA: American Society of Civil Engineers, 2019, 359–370
35. Smith J T, Tighe S L. Assessment of overlay roughness in long-term pavement performance test sites: Canadian case study. Transportation Research Record: Journal of the Transportation Research Board, 2004, 1869(1): 126−135
36. Loizos A, Plati C. An alternative approach to pavement roughness evaluation. International Journal of Pavement Engineering, 2008, 9(1): 69−78
37. Obazee-Igbinedion S O, Owolabi O. Pavement sustainability index for highway infrastructures: A case study of Maryland. Frontiers of Structural and Civil Engineering, 2018, 12(2): 192−200
38. Haas R, Hudson W R, Zaniewski J. Modern Pavement Management. Melbourne, FL: Krieger Publishing Company, 1994
39. Aydın M M, Topal A, Tanyel S. Investigation of the effect of road surface irregularities on driver behavior on multi-lane roads. In: TMMOB 10: Transport Congress, 25–27. Eylül, İzmir, 2013, 413–425 (in Turkish)
40. Terzi S. Modeling for pavement roughness using the ANFIS approach. Advances in Engineering Software, 2013, 57: 59−64
41. Balmer G G. Road Roughness Technology, State of the Art. Final Report, Federal Highway Administration. 1973
42. Quinn B E, Hildebrand S E. The Effect of Pavement Roughness on Safe Vehicle Handling Characteristics. Rept No FHWA-RD-72-25. 1972
43. Chandra S. Effect of road roughness on capacity of two-lane roads. Journal of Transportation Engineering, 2004, 130(3): 360−364
44. Karan M A, Haas R, Kher R. Effects of pavement roughness on vehicle speeds. Transportation Research Record: Journal of the Transportation Research Board, 1976(602): 122−127
45. Yu B, Lu Q. Empirical model of roughness effect on vehicle speed. International Journal of Pavement Engineering, 2014, 15(4): 345−351
46. Hassan R A, McManus K. Assessment of interaction between road roughness and heavy vehicles. Transportation Research Record: Journal of the Transportation Research Board, 2003, 1819(1): 236−243
47. Saplıoğlu M, Aydın M M. Choosing safe and suitable bicycle routes to integrate cycling and public transport systems. Journal of Transport & Health, 2018, 10: 236−252
48. Wang H, Chen Z, Sun L. Pavement roughness evaluation for urban road management. In: Fourth International Conference on Transportation Engineering, Safety, Speediness, Intelligence, Low-Carbon, Innovation. 2013, 2709–2713
49. Hamed K H, Ramachandra Rao A. A modified Mann-Kendall trend test for autocorrelated data. Journal of Hydrology (Amsterdam), 1998, 204(1–4): 182−196
50. Yue S, Hashino M. Long term trends of annual and monthly precipitation in Japan. Journal of the American Water Resources Association, 2003, 39(3): 587−596
51. Şen Z. Trend identification simulation and application. Journal of Hydrologic Engineering, 2014, 19(3): 635−642
52. Mann H B. Non-parametric tests against trend. Econometria, 1945, 13(3): 245−259
53. Kendall M G. Rank Correlation Methods. London: Charles Griffin,

1975

54. Saplıoğlu K. A new methodology for trend analysis: A case study in Burdur and Isparta, Turkey. Fresenius Environmental Bulletin, 2015, 24: 3344−3351
55. Saplıoğlu K, Uzundurukan S. Examination of some artificial intelligence applications and trends used in scientific studies. Journal of Dicle University Engineering Faculty, 2019, 10(1): 249−262
56. Şen Z. Innovative trend analysis methodology. Journal of Hydrologic Engineering, 2012, 17(9): 1042−1046
57. Seo L, Kim T W, Kwon H H. Investigation of trend variations in annual maximum rainfalls in South Korea. KSCE Journal of Civil Engineering, 2012, 16(2): 215−221
58. Saplioglu K, Kilit M, Şenel F. Investigation of changes in climate data using checkerboard: The case of Akarçay basin. Applied Ecology and Environmental Research, 2019, 17(2): 2373−2384